Publication Year	2009
Acceptance in OA@INAF	2023-01-24T11:54:26Z
Title	The dusty nebula surrounding HR Car: A Spitzer view
Authors	UMANA, Grazia Maria Gloria; BUEMI, CARLA SIMONA; TRIGILIO, CORRADO; Hora, J.L.; Fazio, G.G.; et al.
DOI	10.1088/0004-637X/694/1/697
Handle	http://hdl.handle.net/20.500.12386/33031
Journal	THE ASTROPHYSICAL JOURNAL
Number	694

The Astrophysical Journal, 694:697–703, 2009 March 20 doi:10.1088/0004-637X/694/1/697
© 2009. The American Astronomical Society. All rights reserved. Printed in the U.S.A.

THE DUSTY NEBULA SURROUNDING HR CAR: A SPITZER VIEW

G. Umana[1], C. S. Buemi[1], C. Trigilio[1], J. L. Hora[2], G. G. Fazio[2], and P. Leto[3]
[1] INAF-Osservatorio Astrofisico di Catania, Via S. Sofia 75, 95123 Catania, Italy
[2] Harvard-Smithsonian Center for Astrophysics, 60 Garden St. MS-65, Cambridge, MA 02138-1516, USA
[3] INAF-Istituto di Radioastronomia, C.P. 141, Noto, Italy
Received 2008 September 19; accepted 2009 January 2; published 2009 March 17

ABSTRACT

We present mid-IR observations of the Galactic Luminous Blue Variable (LBV) HR Car and its associated nebula carried out with the Spitzer Space Telescope using both Infrared Array Camera and Infrared Spectrograph, as part of a GTO program aimed to study stellar ejecta from evolved stars. Our observations reveal a rich mid-IR spectrum of the inner nebula showing both solid state and atomic gas signatures. Strong low-excitation atomic fine structure lines such as 26.0 μm [Fe II] and 34.8 μm [Si II], indicate, for the first time, the presence of a PDR in this object class. While the physics and chemistry of the low-excitation gas appears to be dominated by photodissociation, a possible contribution due to shocks can be inferred from the evidence of gas phase Fe abundance enhancement. The presence of amorphous silicates, inferred from the observed characteristic broad feature at 10 μm located in the inner nebula, suggests that dust has formed during the LBV outburst. This is in contrast with the detection of crystalline dust in other probably more evolved Galactic LBVs, which is similar to the crystalline dust observed in red supergiants. This has been considered to be evidence of dust production during evolutionary phases prior to the outburst.

Key words: circumstellar matter – infrared: stars – stars: early-type – stars: individual (HR CAR) – stars: winds, outflows

Online-only material: color figures

1. INTRODUCTION

Luminous Blue Variables (LBVs) are luminous, massive stars, which represent a crucial and relatively short phase of massive star evolution between core-hydrogen burning O-type stars and helium burning Wolf–Rayet (W–R) stars. LBVs are quite rare objects in our Galaxy—a recent census reported 12 confirmed members and 23 candidates (Clark et al. 2005). From an observational point of view, LBVs are characterized by strong spectral and photometric variability (van Genderen 2001). Such variability may indicate an increase of the mass-loss rate (Davidson 1987) or a change in the radius of the star (Leitherer et al. 1989). Giant eruptions, during which a large amount of material is released (10^{-5}–10^{-4} $M_{\odot}$yr^{-1}), have been observed between prolonged periods of quiescence. Such events have been witnessed very rarely but the presence of extended circumstellar nebulae (LBVN) around Galactic and extragalactic LBVs suggests that they are a common aspect of LBV behavior (Nota et al. 1992). Most of well known LBVNs contain large quantities of dust: they have been detected by IRAS, ISO, MSX and ground-based near IR imaging as having excess IR and spatially resolved shell images (Trams et al. 1998; Egan et al. 2002; Clark et al. 2003).

According to recent evolutionary models, a massive star has to lose a huge quantity of its main sequence (MS) mass during its post-MS evolution until it reaches its W–R phase during which it completely sheds its H envelope. Lamers et al. (2001) point out that LBVs and related transition objects (Ofpe/WN9 stars), which undergo massive mass-loss and eruptive events, may have a key role in the proposed scenario. There are, however, questions related to LBV phenomenon still under debate and, in particular, the nebula formation mechanism; i.e., the intensity, duration and geometry of single mass-loss event is not yet established. The full characterization of mass-loss properties during the LBV phase appears, therefore, crucial to assess their role in massive star evolution.

Much information on the LBV phenomenon can be derived by the study of the LBVNs, in particular the detailed analysis of gas and dust content in the LBVNs can be used to tackle the problem of their origin. By studying the dust composition, it is possible to observe differences between LBVs that result from differences in the dust forming processes and/or the nebular abundances. The latter, as the dust chemistry would largely reflect the chemical composition of the gas phase, would help in localizing at which phase of stellar evolution the dust has been produced. Moreover, determining the distribution and the morphology of the gas and dust in the nebula may provide clues about the mass-loss history during and/or after the dust formation process.

In order to begin to answer some of these questions, we have started a systematic study of a sample of LBVNs associated with Galactic LBVs using the *Spitzer Space Telescope*. The study is aimed to detect and resolve the faint dust shells that have been ejected from the central stars with mid-IR imaging, and to characterize the mineral composition of LBV ejecta via mid-IR spectra. In this paper we present results on the well-known Galactic LBV HR Car.

1.1. HR Car

HR Car is one of coolest Galactic LBV, classified as B2I. From a spectral analysis of the Balmer lines Manchado et al. (2002) have recently derived a stellar temperature of 10,000 K and a luminosity of 5×10^5 $L_{\odot}$, putting HR Car close to the 40 $M_{\odot}$ evolutionary track in the H–R diagram. The distance to HR Car (5 ± 1 kpc) has been derived by van Genderen et al. (1991), using the reddening-distance method, which is consistent with the value obtained from the kinematic measurements of the Carina spiral arm (5.4 ± 0.4 kpc) by Hutsemkers & Van Drom (1991).

HR Car is surrounded by a faint, low-excitation nebula which is very difficult to observe in the optical due to the strong luminosity of the central object. Despite such difficulties, HR Car and

its associated nebula have been extensively studied. Among the most recent results, Weis et al. (1997) and Nota et al. (1997), both based on optical high resolution coronographic imaging and spectroscopy, found that the nebula has a large-scale bipolar morphology, very reminiscent of the η Carina nebula. Such lobes are expanding in the southeastern–northwestern direction (P.A. = 135°) and have a diameter of ∼18″ (Nota et al. 1997). On a smaller scale of a few arcsecs from the central object, a more compact, brighter nebula is evident, whose morphological details, however, could not be derived from the coronographic optical (H_α) images. Nota et al. (1997) pointed out some degree of asymmetry, especially in the southeastern region of the inner nebula. The presence of some material close to the central object whose distribution is not symmetric was also inferred from the *BVRI* polarization measurements reported by Parthasarathy et al. (2000).

Most of the information on the inner nebula can be obtained at longer wavelengths, where the difficulties due to the contrast between the bright central object and the faint nebula can be overcome. Voors et al. (1997) mapped the dust (broadband 10 μm) and the ionized gas (narrowband [Ne II], 12.8 μm) of the nebula surrounding HR Car. The dusty nebula is quite compact, extending a few arcsecs from the central object, and reveals an asymmetric morphology. The ionized gas has the same extent as the dust, but a different distribution, implying a partial screening of the stellar ionization flux by the circumstellar dust. The most striking result is the difference between the morphology observed at smaller angular scale to that observed in the optical; this may imply that we are tracing different mass-loss episodes, which probably occur with a time-dependent geometry. The same conclusion was reached by White (2000), who observed HR Car with the Australia Telescope Compact Array (ATCA). The radio images reveal an extended ionized region whose morphology closely resembles that of the H_α bipolar nebula plus an inner, compact nebula a few arcsecs across. The inner nebula is strongly asymmetric and in complete disagreement with the large scale structure. Another puzzling feature of this LBV is that the central star does not appear to produce a sufficient quantity of ionizing photons to keep the nebula ionized, even assuming a previous period of higher temperature for the star. A possible explanation that takes in account both the observed degree of ionization and the strong asymmetry of the inner nebula is a symbiotic model, as put forward by White (2000), but the presence of a companion with the required properties has not yet been confirmed.

2. OBSERVATIONS AND DATA REDUCTION

The observations presented in this paper were carried out by using the Infrared Array Camera (IRAC; Fazio et al. 2004) and the Infrared Spectrograph (IRS; Houck et al. 2004) on board the Spitzer Space Telescope (Werner et al. 2004). These observations were part of the GTO program (ID 30188) and were performed on 2006 July 10 (IRAC; AOR 17335040) and 2006 June 28 (IRS; AOR 17335296). Both imaging and spectral observations were obtained at the central source position (R.A.$_{2000}$ = $10^h22^m53^s.84$, decl.$_{2000}$ = $-59^d37^m28^s.4$), which is determined, with good accuracy, from previous IR and radio imaging.

2.1. IRAC 3.6, 4.5, 5.8, and 8.0 μm Images

HR Car was observed with 8 IRAC frames per band using a medium cycling dither pattern at a frame time of 12 s, providing a field of view of approximately 6 × 6 arcmin in the final mosaics.

Table 1
HR Car Fluxes Measured in the IRAC Channels

IRAC Band	Flux Density (Jy)	Mag
3.6	0.985	6.14
4.5	0.848	5.82
5.8	0.714	5.51
8.0	0.910	4.62

The Basic Calibrated Data (BCD) pipeline version S14.0.0 were used in the reduction, and IRACproc (Schuster et al. 2006) was used to create the IRAC final images at a pixel scale of 0.6 arcsec pixel^{-1} (the original IRAC scale is approximately 1.2 arcsec pixel^{-1}). The source structure revealed by previous mid-IR imaging (Voors et al. 1997; Trams et al. 1997) is too compact to be well resolved by IRAC. However, in these observations we are sensitive to fainter emission that is extended further from the star.

At the 12 s frame time, the central star is saturated in all bands in the BCD. The point-spread function (PSF) subtraction technique in IRACproc was used to measure the flux in each of the bands. The PSF-subtracted mosaics are shown in Figure 1, and the flux and magnitudes of the central star are given in Table 1. The PSF-subtracted images have residuals, especially in the central regions, which are in part related to the slightly extended emission around the central star in the mid-IR. The photometry in Table 1 is the flux from the central star only and not the extended emission which is difficult to estimate close to the core. However, one can see evidence in the images for emission on the same spatial scale as seen in the Hα image (Nota et al. 1997), which is brighter at longer IRAC wavelengths.

2.2. IRS Spectra

The spectral observations were obtained by using the Short-High (SH) and Long-High (LH) modules ($R \sim 600$), which cover two spectral ranges going from 9.9 to 19.6 μm (SH) and from 18.7 to 37.2 μm (LH). For each module, three cycles were performed for each nod position in order to provide rejection of cosmic rays and other transient. From the 2D BCD (IRS pipeline version 15.3.0) three spectra, for each nod position, were extracted and wavelength and flux calibrated using the Spitzer IRS Custom Extractor (SPICE) with the extended source extraction option. Using the Spitzer contributed software SMART (Higdon et al. 2004), we cleaned the resulting 1D spectra for residual bad pixels, spurious jumps, and glitches, and smoothed and merged them into one final spectrum per module. The resulting high resolution spectra for each module are shown in Figure 2.

The infrared emission from HR Car consists of narrow emission lines and a solid state feature, at about 10 μm, superimposed on a thermal continuum. There is an expected mismatch between the SH and the LH spectra which is usually attributed to the difference in the two module apertures, as the SH has a slit size of 4.″7 × 11.″3 and the LH has a slit size of 11.″1 × 22.″3. The overplot of the IRS spectral slits for each high resolution module on the Two Micron All Sky Survey (2MASS) K_s (Figure 3) reveals that the central object is well contained in both apertures while only part of the inner nebula is contained in the SH slit. To quantify the correction for aperture losses, we can take advantage of the small spectral overlap between the two modules (from 18.7 to 19.6 μm) deriving a scaling factor of 1.87, at that wavelength range, to align the SH spectrum to the LH spectrum.

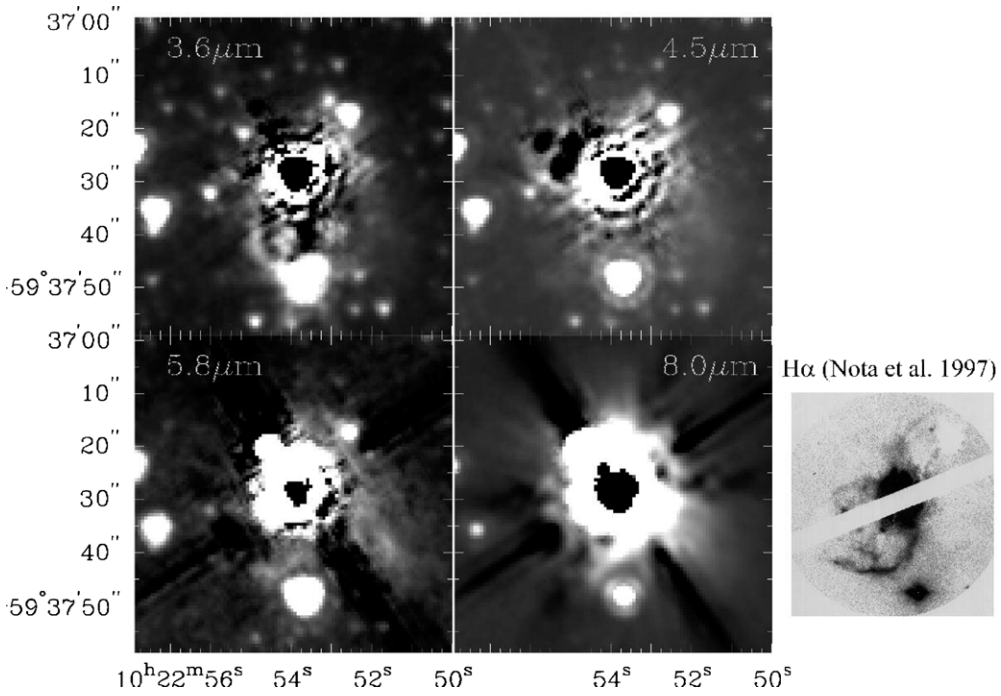

Figure 1. PSF-subtracted images of HR Car based on the 12 sec frames obtained in each of the four IRAC channels. The core of the source was saturated and therefore appears as a black region in the center of the image. The images were rotated approximately 123.3 degrees counterclockwise to align them to R. A. and decl. shown, therefore the array banding, muxbleed, and bandwidth artifacts (Hora et al. 2004) are also rotated from their nominal BCD orientation and appear as dark or bright residuals that are roughly diagonal in the frame. The Hα image from Nota et al. (1997) is shown to the right of the IRAC images. There is low-level extended emission is visible in the images which is similar to that seen in the Hα image. The residual rings near the core result from a mismatch between the PSF and HR Car images, possibly indicating that the core is slightly broader than a point source.

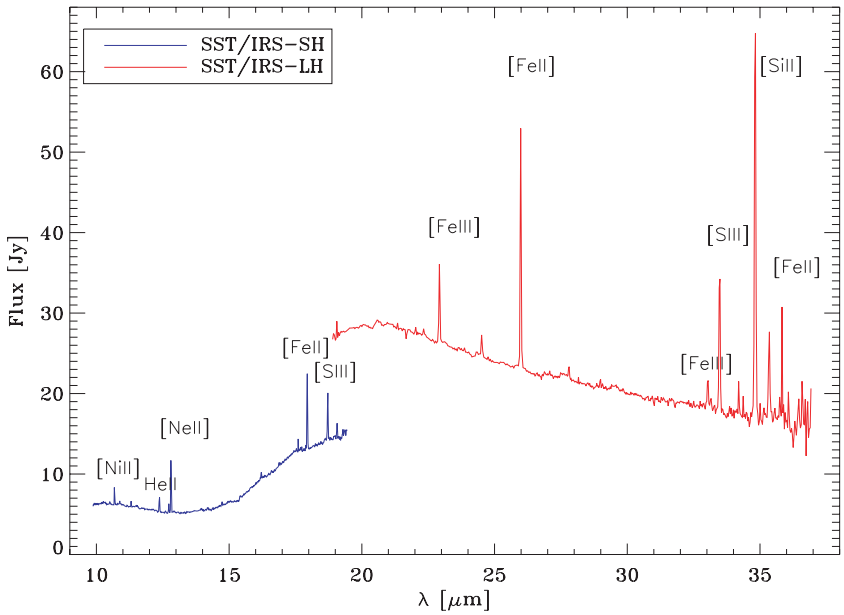

Figure 2. IRS high-resolution spectrum of HR Car.
(A color version of this figure is available in the online journal.)

However, we cannot a priori rule out a wavelength dependence of the missing flux, and a simple scale factor may be an oversimplification. We have therefore retrieved from the ISO Data Archive (IDA v9.0) a Short Wavelength Spectrometer (SWS) spectrum (TDT = 24900321), obtained over the full SWS grating range (2.38–45.2 μm), with a spectral resolution comparable to that of the IRS observations (~600), and with instrumental apertures ranging from 14″ × 20″ (2.4–12 μm) to 20″ × 33″ (29–45 μm). Therefore, in the SWS observations the whole inner nebula was included in the aperture. This spectrum was already presented by Lamers et al. (1996), but the data we retrieved from the archive are the result of further processing beyond the original pipeline with new, more refined algorithms (Highly Processed Data Products), providing a much improved spectrum with respect to the published one (Sloan et al. 2003).

In Figure 4 the two Spitzer-IRS spectra are superimposed on the ISO data. A good agreement is evident up to ~10 μm. After that, there is a mismatch, with the amplitude increasing with

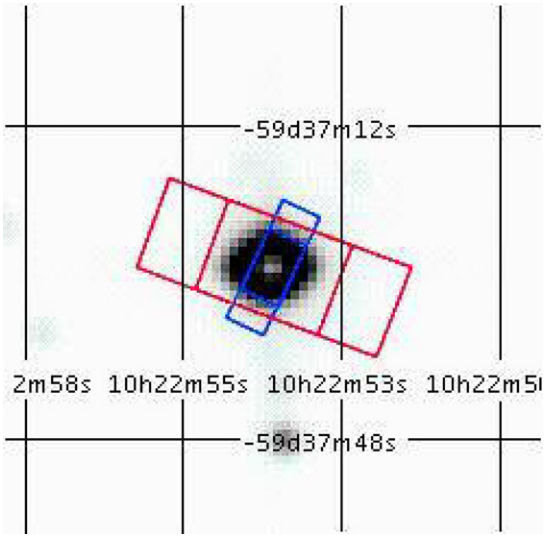

Figure 3. Overplot of the IRS spectral slits, for both high resolution modules, on the 2MASS K_s image. The smaller aperture (blue box in the electronic edition) corresponds to the SH aperture, the larger one (red box in the electronic edition) is the LH aperture.

(A color version of this figure is available in the online journal.)

wavelength, indicating that a simple scale factor cannot account for aperture losses. The IRS-LH is again in good agreement with the ISO spectrum up to ∼27 μm. At higher wavelengths in the ISO spectrum, there are additional apparent features which have been reported by Lamers et al. (1996), but these features are completely absent in the IRS spectrum. We will further discuss the implications of these observed differences between the spectra in the following section.

3. SOLID STATE FEATURES

The mid-IR spectrum of HR Car reveals a prominent feature that peaks at around 10 μm that is probably related to the 9.7 μm feature due to the Si–O stretching mode in amorphous silicates. This feature was also noted by Lamers et al. (1996). The presence of amorphous silicate in the stellar ejecta indicates an oxygen-rich (C/O $\leqslant$ 1) environment, as we expect for LBV ejecta being enriched by CNO processed material (Nota et al. 1997).

In the comparison of the IRS spectrum with the ISO SWS spectrum (Figure4), we notice a reasonably good match between the two spectra at around 10 μm. Since the two instruments have different apertures, the fact that in both spectra we see the same features with the same intensity implies that amorphous silicates must form very close to the central object, well inside the inner nebula, in a region whose extension must be comparable to or less than the IRS-SH aperture. At longer wavelenghts, we find that in the ISO spectrum there is a strong contribution beyond 27 μm that is completely absent in the IRS spectrum. However the ISO spectrum is quite noisy in that wavelength range and it is difficult to assess the reliability of the observed broad structures. If we assume that the observed difference is related to the aperture, we may conclude that the emission features arise from a region located outside of the inner nebula, otherwise it should have been detected in the IRS spectrum. The features must be present in a region which is, at least partly, inside the area seen by the SWS aperture. The nature of such a contribution is not clear. Lamers et al. (1996) and Waters et al. (1997) indicate a solid state origin, but no firm conclusion on the possible carrier/s was reached.

At this time, we can only speculate on the possible location of this material, but we cannot discriminate whether the spectral features are connected to some outer region of the HR Car nebula or to the interstellar medium (ISM) surrounding it.

4. THE EMISSION LINE SPECTRUM

The mid-IR spectrum of HR Car shows many fine structure lines that, once the mechanisms responsible of the observed emission have been identified, may provide important constraints on the physical conditions in the line emitting region. The line-fitting routine in SMART was used to identify and measure the narrow lines. For each line a local continuum was defined by a single-order fit to the baseline and the line was then fitted using a single Gaussian.

The most prominent lines are labeled in Figure 2, while the identification and the measured fluxes, including weaker lines (S/N $\leqslant$ 20) are summarized in Table 2. Possible multiple identifications are also indicated. High ionization potential lines such as those of [S III] and [Fe III] can only originate in the H II region around the star, while the fine structure lines such as those of [Fe II] and [Si II] can form in a photodissociation region (PDR) surrounding the ionized part of the LBVN, where the gas is predominantly neutral but whose chemistry and thermal balance is controlled by FUV photons, i.e., with energies between 6 and 13.6 eV (Tielens & Hollenbach 1985). PDRs are bright in the far-IR dust continuum, in the polycyclic aromatic hydrocarbon (PAH) emission features, in some infrared fine-structure lines and in rotational lines of CO. CO emission detected in other LBV (Nota et al. 2002; Rizzo et al. 2008) supports the hypothesis of the presence of PDRs in the LBVNs.

4.1. [S III] Lines

The [S III] 33.48 μm and [S III] 18.71 μm lines can be used to derive the electron density in the ionized nebula associated with HR Car. Those lines originate from levels close in energy, and therefore their ratio will have almost no dependence on temperature, being only sensitive to their transition probabilities or collisional de-excitation, which depend on density.

The [S III] 18.71 μm line is located in the overlap between the two high resolution modules. We can therefore safely apply the correction factor of 1.87 to take the aperture losses into account. From the observed ratio of the 33.48 μm line flux to the 18.71 μm line flux, we derive, assuming a electronic temperature of $T_e \sim 10^4$ K, an electronic density of the H II region $n_e \geqslant 10^3$ cm^{-3} (Houck et al. 1984). Because this line ratio is insensitive to temperature, the adopted value of T_e will not affect the value of n_e. The derived value of n_e is in good agreement with those derived by Nota et al. (1997), who obtained, from [S II] line ratios, a gradient in the electron density n_e ranging from ∼10^4 cm^{-3} in the center of the nebula to a value of ∼10^3 cm^{-3} at a distance from the core of ∼5″. A similar value for the electron density ($n_e = 3200$ cm^{-3}) was derived from the central core of the ionized nebula (6″ × 8″) by White (2000) from radio measurements.

The agreement of our density determination with those derived by other authors in other spectral regions also supports the adopted scaling factor applied to the SH spectrum to account for aperture losses. The noncorrected 18.71 μm line flux would lead to a [S III] lines ratio that implies a very low density H II region ($n_e = 10$–100 cm^{-3}), which is not consistent with results from visible and radio observations.

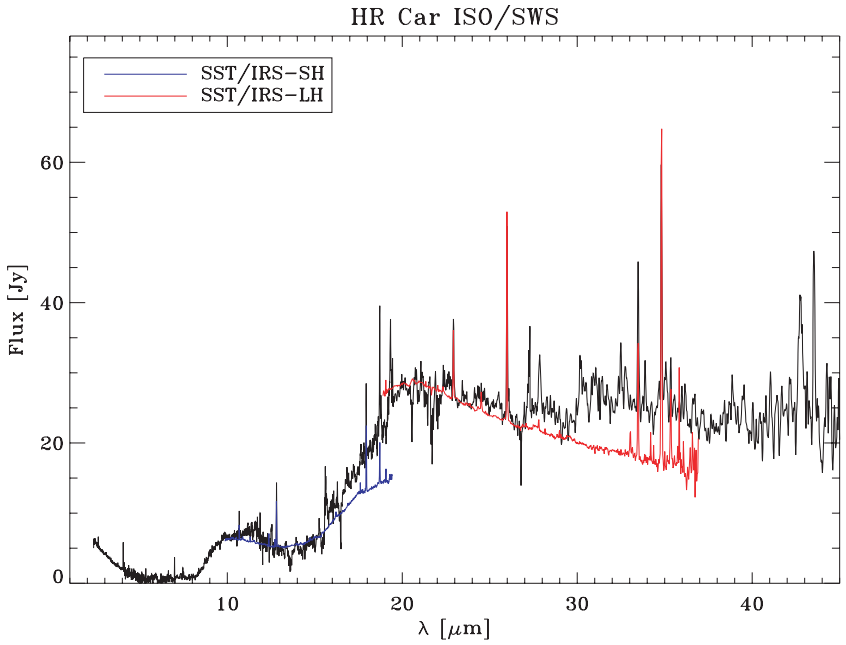

Figure 4. IRS/SH and LH spectra superimposed to the ISO-SWS01 archive spectrum.
(A color version of this figure is available in the online journal.)

Table 2
Line Identifications and Measured Fluxes

Identification	$\lambda(\mu m)$	Flux[a]
[Ni II]	8.68	193[b]
He II/Si IV	10.49	29[c]
H I	10.85	29[c]
He II	11.30	12[c]
He II	12.30	124[b]
[Ni II]	12.72	50[c]
[Ne II]	12.81	374[b]
[Co II]	14.74	14[b]
He II/H I	16.29	46[c]
H I	17.60	8.2[c]
[Fe II]	17.93	268[b]
[S III]	18.71	303[b,d]
H I	19.04	50[c]
[Fe III]	22.92	255[b]
[N V]	24.31	18[c]
[Fe II]	24.51	84[b]
[Fe II]	25.98	594[b]
H I	27.80	25[c]
[Fe III]	33.03	50[b]
[S III]	33.48	280[b]
[Si II]	34.81	813 [b]
[Fe II]	35.34	157[b]

Notes.
[a] Observed fluxes in units of 10^{-14}erg cm^{-2} s^{-1}.
[b] Flux uncertainties $\leqslant$ 10%.
[c] Flux uncertainties between 10% and 20%.
[d] The measured flux has been corrected for the scale factor 1.87.

4.2. [Fe II] and [Si II] Lines

The [Fe II] 26.0 μm and [Si II] 34.8 μm lines may arise from the ionized region of the LBVN (H II region) and/or from the associated PDR. Therefore, we cannot a priori exclude a mixed contribution from these different regions to the observed line intensities. The use of these lines as diagnostics of the physical condition in the PDR is limited by the knowledge of the real PDR contribution. In a recent paper, Kaufman et al. (2006) modeled the intensities of typical infrared fine-structure lines that may originate from both the H II region and the associated PDR in order to evaluate the contribution to such diagnostics from the two different regions. They concluded that, in the hypothesis of thermal pressure balance between the H II regions and the PDR and normal metallicity, the fine structure line of [C II] at 158.0 μm is always dominated by the PDR, while the [Fe II] 26.0 μm and [Si II] 34.8 μm emission is dominated by the PDR if the H II region has a high electron density $n_e \geqslant 10\,\mathrm{cm}^{-3}$. A similar conclusion was reached by Abel et al. (2005).

Assuming the n_e for the H II region associated with HR Car as derived from the [S III] line ratio, we conclude that the [Fe II] 26.0 μm and [Si II] 34.8 μm lines observed in the mid-IR spectrum of HR Car are PDR-dominated and can be safely used to derive the physical conditions of this region. For this purpose we need to compare the observed line intensities with those predicted by the theoretical PDR models.

The physics and chemistry of a PDR are governed by the incident FUV (6 eV $\leqslant h\nu \leqslant$ 13.6 eV) radiation, often expressed as relative to the background interstellar radiation field assumed to be 1.6×10^{-3} erg cm^{-2} s^{-1}

$$G_o = \frac{\int_{912\text{Å}}^{2067\text{Å}} I_\lambda d\lambda}{1.6 \times 10^{-3} (\mathrm{erg\,cm^{-2} s^{-1}})} \quad (1)$$

and by the total density n_o (cm^{-3}).

In Figures 5 and 6, the line intensities for [Si II] 34.8 μm and [Fe II] 26.0 μm computed with the model of Kaufman et al. (2006) are shown as function of G_o for several values of n_o. The measured fluxes of the [Fe II] 26.0 μm and [Si II] 34.8 μm lines correspond to a line intensity of 1.04×10^{-3} (erg cm^{-2} s^{-1} sr^{-1}) and 1.42×10^{-3}(erg cm^{-2} s^{-1} sr^{-1}) respectively, if we assume that the PDR completely fills the LH aperture ($\Omega_{\mathrm{PDR}} = 0.57 \times 10^{-8}$ sr). The shaded regions in each figure indicate our line measurement with the associated uncertainty.

Different combinations of the space parameters (G_o, n_o) can explain the observed line intensity of [Si II] at 34.8 μm, going

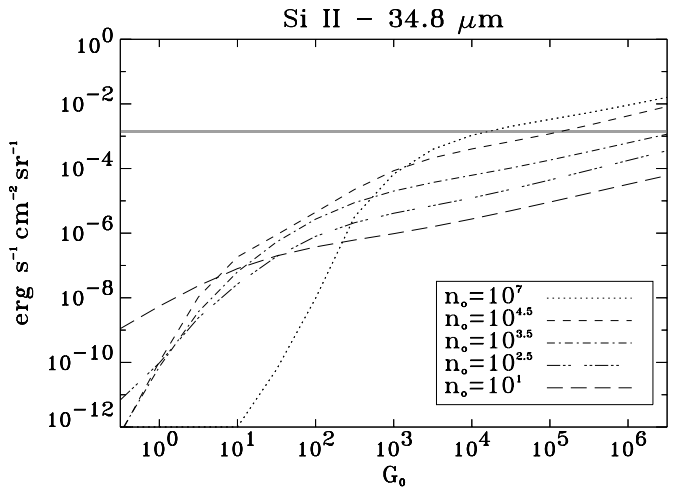

Figure 5. Line intensity for [Si II] 34.8 μm computed with the model of Kaufman et al. (2006) is shown as function of G_o for several values of n_o. The shaded region indicates our line measurement with associated uncertainty.

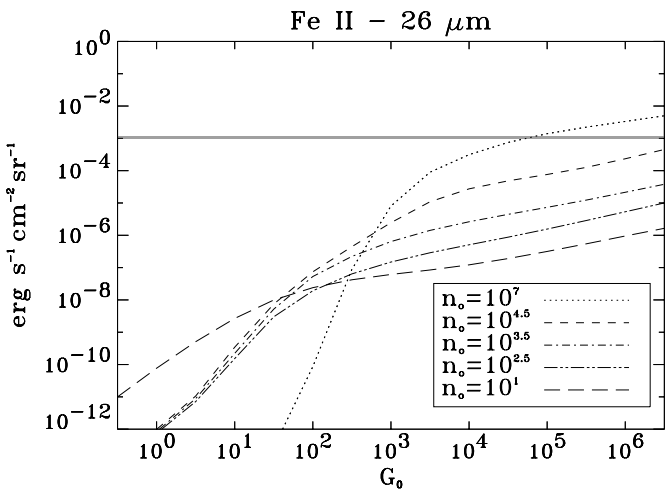

Figure 6. Same as Figure 5 but for [Fe II] 26.0 μm line.

from a high density ($n_o \sim 10^6$) and a moderate incident FUV radiation $\log(G_o) \sim 3.5$ to a low density ($n_o \sim 10^{3.5}$) and a high incident FUV radiation $\log(G_o) \sim 6$ (Figure 5). On the other hand, to explain the observed line intensity of [Fe II] at 26.0 μm, a very high density ($n_o \geqslant 10^7$) and a high incident FUV radiation ($\log(G_o) \geqslant 4.5$) are necessary.

Because the [Fe II] line at 26.0 μm and the [Si II] line at 34.8 μm are optically thin (Tielens & Hollenbach 1985), the modeled line intensities scale linearly with the adopted gas phase abundance. This means that to have physical conditions of the PDR consistent with both the observed line intensities, the gas phase Fe abundance in the nebula should be higher than the values adopted by the Kaufman et al. (2006) standard model typical for the diffuse ISM (1.7×10^{-7}).

It is quite difficult to quantify the gas phase Fe abundance necessary to reproduce the observed 26.0 μm [Fe II] line intensity without detailed modeling. The PDR model of Tielens & Hollenbach (1985), which assumes a gas phase Fe abundance of 2.5×10^{-7}, foresees a 26.0 μm [Fe II] line intensity of 4×10^{-4}erg cm^{-2} s^{-1} sr^{-1}, for $G_o = 10^5$ and $n_o = 10^{4...5}$. Therefore, with an increment of ~50% of the gas phase Fe abundance, the expected 26.0 μm [Fe II] line intensity is enhanced of a factor of four, shifting the model curves shown in Figure 6 toward our observed values.

5. CONCLUSIONS

We have presented mid-IR observations of the Galactic LBV HR Car and its associated nebula carried out with Spitzer using both IRAC and IRS, as part of a GTO program aimed to study stellar ejecta from evolved stars.

The central object in HR Car is too bright in the mid-IR and the warmer inner dusty nebula too compact to get reliable mapping with IRAC; still, the adopted observing strategy has allowed us to observe the presence of faint structures, brighter at longer IRAC wavelengths, whose extension is comparable to those of inner ionized nebula traced by H_α and the radio. The more extended nebula, which, in the mid-IR, can be detected only through its free–free continuum (no strong recombination lines are evident in the ISO spectrum for $\lambda \leqslant 10\,\mu$m), is expected to be too faint to be observable at the integration time used.

We have further obtained a mid-IR spectrum of the inner nebula and a few arcsecs across the central object. The spectrum reveals quite a number of emission lines, some of which are formed in the ionized part of the nebula. Particularly interesting is the presence of low-excitation atomic fine structure lines such as 26.0 μm [Fe II] and 34.8 μm [Si II], lines whose detection may indicate the presence of a PDR. The comparison between the observed line intensities and those derived from recent PDR models supports the existence of a PDR surrounding the ionized fraction of the nebula. However, to obtain a PDR with physical characteristics that are able to reproduce both [Fe II] and [Si II] line intensities, a Fe gas phase abundance higher than that of the ISM is necessary.

In the ISM, Fe is usually highly depleted from the gas phase because of condensation onto dust grains. In this context, a higher Fe gas phase abundance with respect to that of the ISM may be considered as indirect evidence of shocks occurring in the nebula resulting in grain processing that release Fe atoms into the gas phase.

Such an enhanced Fe abundance has been observed in the radio Arc Bubble of the Galactic Center and has been interpreted in terms of additional Fe released to the gas phase as a consequence of grain destruction by shocks (Simpson et al. 2007). Such shocks are probably produced in the strong stellar winds of the Quintuplet Cluster stars, which also includes a LBV, the Pistol star. Shock heating has been proposed by Smith (2002) to explain the bright 1.643 μm [Fe II] line observed in a small sample of LBVs. While the presence of such a line seems to be a common property of LBV nebulae, its possible excitation mechanism has not been clearly established. We conclude that in the case of HR Car, the photodissociation dominates the physics and the chemistry of its outer envelope, but shocks also play an important role as inferred from the enhanced gas phase Fe abundance.

The analysis of the IRS spectrum has allowed us to derive some clues on the mineralogy and spatial distribution of the dust. There is a strong signature of amorphous silicate, which appears to be localized within ~10″ (0.3 pc, assuming a distance of 5.4 kpc) from the central object, in a region spatially coincident with the optical, IR, and radio inner nebula. Our result is consistent with the amorphous silicates being localized in the compact (~3″) nebula mapped at 10 μm by Voors et al. (1997). Such a strong emission band is probably also responsible for the diffuse emission detected in the $8.0 \pm 1.5\,\mu$m IRAC band. The spatial coincidence among the IRAC structures with the inner H_α nebula reported by Nota et al. (1997) and Weis et al.

(1997) strongly supports our conclusion that ionized gas and amorphous silicate are localized within the same area.

Relative to the region of the nebula covered by the IRS apertures, we cannot confirm the presence of crystalline features indicated by previous ISO observations. The presence of amorphous silicates, together with the lack of crystalline silicates in the inner part of the nebula, suggest that there has been recent dust formation in HR Car that has condensed during the LBV eruptions. This is in contrast with other Galactic LBVs, such as AR Car and WR751, where crystalline dust has been observed. The similarity of the crystalline dust in those objects to the dust observed in red supergiants has been considered evidence of dust production in a previous evolutionary phase of these massive stars, prior to the LBV outbursts (Waters et al. 1998).

We thank the referee for her/his comments and suggestions. This work is based in part on observations made with the *Spitzer Space Telescope*, which is operated by the Jet Propulsion Laboratory, California Institute of Technology under NASA contract 1407. Support for this work was provided by NASA through Contract Number 1256790 issued by JPL/Caltech. Support for the IRAC instrument was provided by NASA through Contract Number 960541 issued by JPL. The IRS was a collaborative venture between Cornell University and Ball Aerospace Corporation funded by NASA through the Jet Propulsion Laboratory and Ames Research Center. SMART was developed at Cornell University and is available through the Spitzer Science Center at Caltech. This publication makes use of data products from the 2MASS, which is a joint project of the University of Massachusetts and the Infrared Processing and Analysis Center/California Institute of Technology, funded by the National Aeronautics and Space Administration and the National Science Foundation.

Facilities: Spitzer (IRAC), *Spitzer* (IRS).

REFERENCES

Abel, N. P., Ferland, G. J., Shaw, G., & van Hoof, P. A. M. 2005, ApJS, 161, 65
Clark, J. S., Egan, M. P., Crowther, P. A., Mizuno, D. R., Larionov, V. M., & Arkharov, A. 2003, A&A, 412, 185
Clark, J. S., Larionov, V. M., & Arkharov, A. 2005, A&A, 435, 239
Davidson, K. 1987, ApJ, 317, 760
Egan, M. P., Clark, J. S., Mizuno, D. R., Carey, S. J., Steele, I. A., & Price, S. D. 2002, ApJ, 572, 288
Fazio, G. G., et al. 2004, ApJS, 154, 10
Higdon, S. J. U., et al. 2004, PASP, 116, 975
Hora, J. L., et al. 2004, Proc. SPIE, 5487, 77
Houck, J. R., Shure, M. A., Gull, G. E., & Herter, T. 1984, ApJ, 287, L11
Houck, J., et al. 2004, ApJS, 154, 18
Hutsemkers, D., & Van Drom, E. 1991, A&A, 248, 141
Kaufman, M. J., Wolfire, M. G., & Hollenbach, D. J. 2006, ApJ, 644, 283
Lamers, H. J. G. L. M., et al. 1996, A&A, 315, L225
Lamers, H. J. G. L. M., Nota, A., Panagia, N., Smith, L. J., & Langer, N. 2001, ApJ, 551, 754
Leitherer, C., Schmutz, W., Abbott, D. C., Hamann, W.-R., & Wessolowski, U. 1989, ApJ, 346, 919
Manchado, M. A. D., Araujo, F. X., Pereira, C. B., & Fernandes, M. B. 2002, A&A, 387, 151
Nota, A., Pasquali, A., Marston, A. P., Lamers, H. J. G. L. M., Clampin, M., & Schulte-Ladbeck, R. E. 2002, AJ, 124, 2920
Nota, A., Smith, L., Pasquali, A., Clampin, M., & Stroud, M. 1997, ApJ, 486, 338
Nota, A., Leitherer, C., Clampin, M., Greenfield, P., & Golimowski, D. A. 1992, ApJ, 398, 621
Parthasarathy, M., Jain, S. K., & Bhatt, H. C. 2000, A&A, 355, 221
Rizzo, J. R., Jimenez-Esteban, F. M., & Ortiz, E. 2008, ApJ, 681, 355
Schuster, M. T., et al. 2006, Proc. SPIE., 6270, 627020
Simpson, J. P., Colgan, S. W. J., Cotera, A. S., Erickson, E. F., Hollenbach, D. J., Kaufman, M. J., & Rubin, R. H. 2007, ApJ, 670, 1115
Sloan, G. C., Kraemer, K. E., Price, S. D., & Shipman, R. F. 2003, ApJS, 147, 379
Smith, N. 2002, MNRAS, 336, L22
Tielens, A. G. G. M., & Hollenbach, D. J. 1985, ApJ, 291, 722
Trams, N. R., Voors, R. H. M., & Waters, L. B. F. M. 1998, Ap&SS, 255, 195
Trams, N. R., Waters, L. B. F. M., & Voors, R. H. M. 1997, in ASP Conf. Ser. 120, Luminous Blue Variables: Massive Stars in Transition, ed. A. Nota & H. J. G. L. M. Lamers (San Francisco, CA: ASP), 351
van Genderen, A. M. 2001, A&A, 366, 508
van Genderen, A. M., Robijn, F. A. H., van Esch, B. P. M., & Lamers, H. J. G. L. M. 1991, A&A, 246, 407
Voors, R. H. M., Waters, L. B. F. M., Trams, N. R., & Käufl, H. U. 1997, A&A, 321, L21
Waters, L. B. F. M., Morris, P. W., Voors, R. H. M., Lamers, H. J. G. L. M., & Trams, N. R. 1998, Ap&SS, 255, 179
Waters, L. B. F. M., Morris, P. W., Voors, R. H. M., & Lamers, H. J. G. L. M. 1997, in ASP Conf. Ser. 120, Luminous blue variables: massive stars in transition, ed. A. Nota & H. J. G. L. M. Lamers (San Francisco, CA: ASP), 326
Werner, M., et al. 2004, ApJS, 154, 1
Weis, K., Duschl, W. J., Bomans, D. J., Chu, Y. H., & Joner, M. D. 1997, A&A, 320, 568
White, S. M. 2000, ApJ, 539, 851